



NOTE

Pathology

Immunohistochemical analysis of periostin in the hearts of Lewis rats with experimental autoimmune myocarditis

Yuna CHOI^{1) #}, Hanseul OH^{2) #}, Meejung AHN³⁾, Taeyoung KANG¹⁾, Jiyeon CHUN¹⁾, Taekyun SHIN^{1) *} and Jeongtae KIM^{4) *}

¹⁾College of Veterinary Medicine and Veterinary Medical Research Institute, Jeju National University, Jeju 63243, Republic of Korea

²⁾National Primate Research Center, Korea Research Institute of Bioscience and Biotechnology, Cheongju 28116, Republic of Korea

³⁾Department of Animal Science, College of Life Science, Sangji University, Wonju 26339, Republic of Korea

⁴⁾Department of Anatomy, Kosin University College of Medicine, Busan 49267, Republic of Korea

J. Vet. Med. Sci.
82(10): 1545–1550, 2020
doi: 10.1292/jvms.20-0225

Received: 19 April 2020
Accepted: 20 July 2020
Advanced Epub:
5 August 2020

ABSTRACT. Periostin plays a critical role in tissue regeneration and homeostasis. The aim of this study was to evaluate the changes in periostin levels in the hearts of rats with experimental autoimmune myocarditis (EAM). Western blot analysis revealed that the expression levels of periostin and alpha-smooth muscle actin were significantly increased at day 14 post-immunization. Immunohistochemical analysis indicated that periostin was expressed in macrophages and fibroblasts in the hearts of EAM-induced rats. In conclusion, these results suggest that increased periostin expression in macrophages and fibroblasts promotes cardiac fibrosis in EAM-induced rats, potentially by enhancing immune cell infiltration. Therefore, periostin should be further investigated as a candidate therapeutic target for myocarditis.

KEY WORDS: autoimmune disease, fibrosis, myocarditis, periostin, smooth muscle actin

Periostin, also referred to as osteoblast-specific factor (OSF)-2, is the representative extracellular matrix component secreted primarily by fibroblasts and macrophages [21]. Under physiological conditions, periostin promotes tissue development and regeneration in several tissues and organs, including bones [14], heart [15], and the central nervous system [20]. Furthermore, periostin has been implicated in tumorigenesis [15], cell migration during the inflammatory responses [11] and fibrosis [10]. Periostin plays diverse roles in cell migration and tissue repair in various diseases and conditions, including autoimmune myocarditis [8].

Rodent experimental autoimmune myocarditis (EAM) models are widely used to study human giant cell myocarditis, a type of autoimmune inflammatory cardiac disorder mediated by excessive infiltration of T cells [12] and macrophages [4]. Immune cell infiltration and fusion can promote cardiac myocyte loss and fibrosis, potentially leading to cardiac dysfunction [15, 16]. Even though the importance of fibroblasts in myocarditis has been shown both in human myocarditis and in animal EAM models, the EAM-associated changes in periostin in the heart remain elusive. The aim of this study was to evaluate the changes in periostin levels and cellular sources in the heart in EAM-associated fibrosis.

Male Lewis rats (10 weeks old) were obtained from Orientbio Inc. (Gyeonggi-do, Korea) and housed in our facility under controlled conditions (12-hr light/dark cycle, temperature $24 \pm 2^\circ\text{C}$). All animal protocols conformed to international laws and NIH policies, including the Care and Use of Laboratory Animals (NIH publication no. 85-23, 1985 edition). All experimental procedures were performed in accordance with the Guidelines for the Care and Use of Laboratory Animals of Jeju National University (Permission Number 2019-0027).

Induction of EAM was performed as described previously [1, 19]. Briefly, the hind soles of rats were injected with $200 \mu\text{l}$ of human cardiac myosin (2 mg/ml) mixed with an equal volume of complete Freund's adjuvant supplemented with 5 mg/ml *Mycobacterium tuberculosis* H37RA (Difco, Detroit, MI, USA). Experimental animals were intraperitoneally administered with 500 ng of pertussis toxin (List Biological Laboratories, Inc., Campbell, CA, USA) on the day of immunization day 0 and 2 days post-immunization (D2PI). Control and EAM-induced rats were sacrificed under deep anesthesia with diethyl ether on D14PI, D21PI, or D28PI ($n=5/\text{groups}$).

*Correspondence to: Kim, J.: kimjt78@kosin.ac.kr, Shin, T.: shint@jejunu.ac.kr

#These authors contributed equally to this work.

©2020 The Japanese Society of Veterinary Science



This is an open-access article distributed under the terms of the Creative Commons Attribution Non-Commercial No Derivatives (by-nc-nd) License. (CC-BY-NC-ND 4.0: <https://creativecommons.org/licenses/by-nc-nd/4.0/>)

Rat tissues were harvested and fixed for 48 hr in 4% (v/v) paraformaldehyde in phosphate buffered saline (PBS; pH 7.2). Hearts were embedded in paraffin wax, and 5- μ m-thick sections were prepared using a rotary microtome (RM 2135; Leica, Nussloch, Germany). Heart sections were stained with hematoxylin and eosin (H&E). Masson's trichrome staining [7] and Sirius red staining (Direct Red 80, Sigma-Aldrich, St. Louis, MO, USA) were also performed to evaluate for fibrosis.

Protein samples were separated by SDS-PAGE and transferred onto nitrocellulose membranes (Schleicher and Schuell, Keene, NH, USA). Membranes were incubated with the following primary antibodies: rabbit anti-periostin (1:500, ab14041, Abcam), mouse anti- α smooth muscle actin (α SMA; 1:1,000, A2547, Sigma-Aldrich), and rabbit anti-glyceraldehyde-3-phosphate dehydrogenase (GAPDH; 1:1,000, SC-25778, Santa Cruz Biotechnology, Santa Cruz, CA, USA). Thereafter, membranes were incubated with the appropriate horseradish peroxidase (HRP)-conjugated secondary antibody (Vector Laboratories, Burlingame, CA, USA) and visualized using a chemiluminescence kit (BS ECL Plus Kit, W6002; Biosesang, Gyeonggi, Korea). Signal intensities were analyzed using FUSION Solo 6X software (Vilber Lourmat, Collegien, France). Band intensities were normalized to GAPDH. All measurements are averages of three independent experiments. All values were expressed as mean \pm standard error of the mean (SEM). Data were analyzed using one-way analysis of variance (ANOVA) followed by Student-Newman-Keuls posthoc testing for multiple comparisons. *P* values <0.05 were considered statistically significant.

Immunohistochemistry was performed using the avidin-biotin complex method (Vectastain Elite ABC Kit; Vector Laboratories) as described in our previous study [13]. Rabbit anti-periostin and mouse anti- α SMA were used as primary antibodies. Sections were then incubated with the appropriate biotinylated secondary antibody. Peroxidase activity was determined using diaminobenzidine (DAB) substrate (Vector Laboratories).

Double immunofluorescence staining was performed as previously described [13]. Sections were incubated overnight at 4°C with rabbit anti-periostin. Subsequently, sections were incubated with fluorescein isothiocyanate (FITC)-labeled goat anti-rabbit IgG (1:50, Sigma-Aldrich). Sections were then incubated overnight with the following primary antibodies: mouse monoclonal anti-rat CD68 (ED1; 1:800, MCA341, Serotec, Kidlington, UK), mouse anti- α SMA (fibroblast marker; 1:4,000, A2547, Sigma-Aldrich), or isolectin-B4 (IB4) (macrophage and vascular endothelial marker; 1:100, L-2140, Sigma-Aldrich). After incubation with primary antibodies, the sections were incubated with tetramethylrhodamine isothiocyanate-conjugated horse anti-mouse IgG (1:50; Sigma-Aldrich) or tetramethylrhodamine isothiocyanate-labeled streptavidin (1:500; Jackson ImmunoResearch Labs, West Grove, PA, USA). Immunofluorescent images were merged using Adobe Photoshop (Adobe Systems, San Jose, CA, USA).

The enlarged heart of EAM-induced rat was shown the discolored surface, compared to that of normal control (Fig. 1A). The body weight of EAM-affected rats was significantly lower, commencing on D10PI (*P*<0.05), than that of normal control rats (Fig. 1B). Although inflammatory cells were absent in the hearts of control rats (Fig. 2A), the hearts of EAM-affected rats were infiltrated with inflammatory cells at D14PI (Fig. 2B and 2C). At D28PI, fibrotic lesions were evident in the hearts of EAM-induced rats, while some inflammatory cells were still present (Fig. 2D and 2E). The intensity of Masson's trichrome stain was higher in the hearts of EAM-induced rats at D14PI (Fig. 2G) compared with control hearts (Fig. 2F). At D28PI (Fig. 2H), the hearts of EAM-induced rats exhibited larger fibrotic lesions (arrowheads in Fig. 2H) than at D14PI (Fig. 2G). The presence of fibrosis in the hearts of EAM-induced rats (arrows in Fig. 2K) was confirmed by Sirius red staining (Fig. 2I–K).

Periostin expression levels in the hearts of EAM-induced rats at D14PI (1.42 \pm 0.17 fold change, optical density/mm²) were

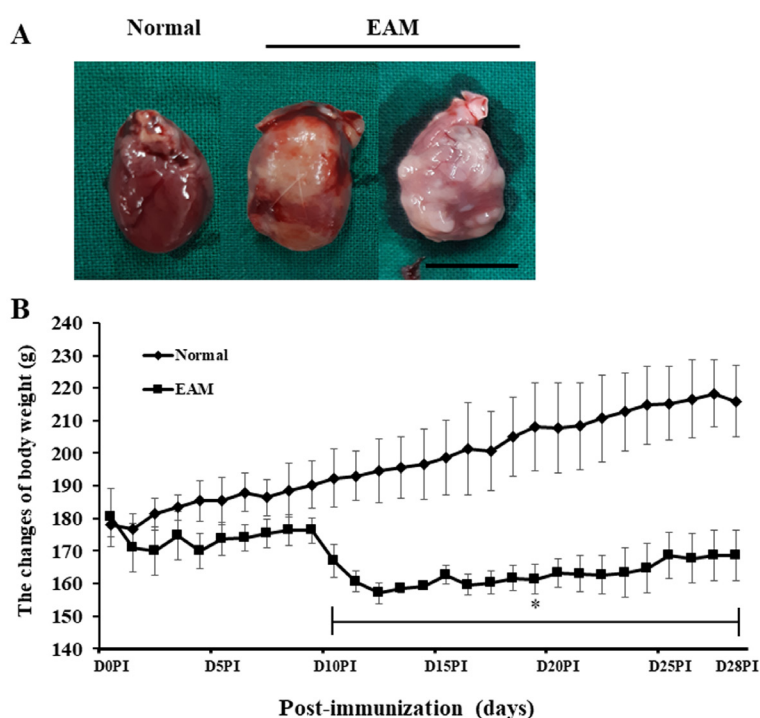


Fig. 1. The representative photos and body weights of normal control and experimental autoimmune myocarditis (EAM)-induced rats. (A) Heart of experimental autoimmune myocarditis (EAM)-induced rats were shown the discolored surface and enlarged, compared to that of normal controls. (B) The body weight significantly decreased in EAM-induced rats from day 10 post-immunization, compared to that of normal controls. Rats were weighed daily. **P*<0.05 vs. control. (A) Scale bar, 1 cm.

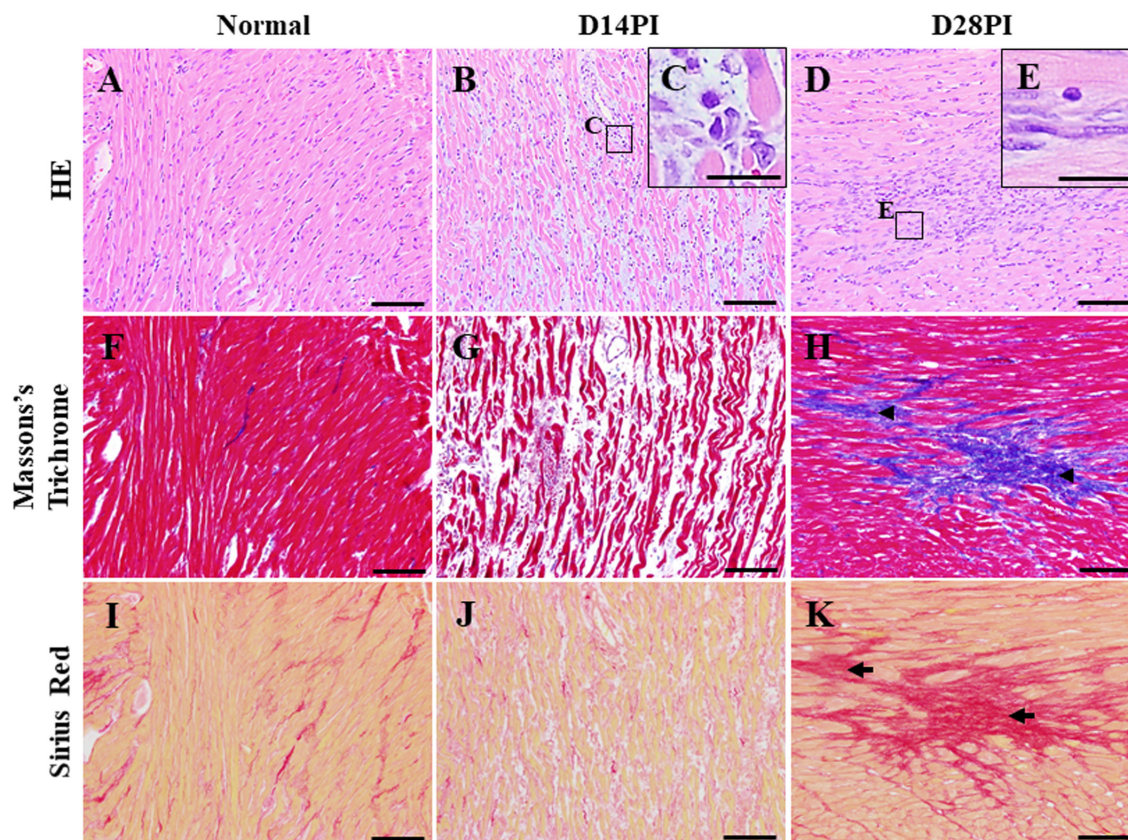


Fig. 2. Histopathological evaluation of the fibrosis in heart of normal (A) and experimental autoimmune myocarditis (EAM)-affected rats (B and D). The normal rat heart contained no inflammatory cells (A), but such cells were evident in the EAM-affected heart (B and D). The insets (C and E) show inflammatory cells under high magnification. Fibrotic lesions (arrowheads indicating blue in F–H; arrows indicating red in K) were detected in the hearts of EAM-affected rats. (A–E) Hematoxylin-and-eosin staining. (F–H) Masson's Trichrome staining. (I–K) Sirius Red staining. HE, Hematoxylin-and-eosin staining; D14PI, day 14 post-immunization; D28PI, day 28 post-immunization. (A, B, D, F, G, H, I, J and K) Scale bars, 100 μm . (C and E) Scale bars, 20 μm .

significantly higher compared with those in the hearts of control rats (1.00 ± 0.07 , $P < 0.05$; Fig. 3A and 3B). The expression levels of periostin were further increased during EAM progression (D21PI, 6.17 ± 1.12 , $P < 0.01$ vs. control; D28PI, 9.48 ± 1.86 , $P < 0.001$ vs. control). Furthermore, the expression pattern of αSMA was similar to that of periostin during EAM progression (Fig. 3A and 3C). Immunohistochemical stainings revealed that periostin was expressed at low levels in fibroblasts of control rats (Fig. 4A). On the other hand, periostin was strongly expressed in inflammatory cells and the fibrotic lesions (including the fibrotic stroma and fibroblasts) of EAM-induced rats on D14PI (Fig. 4B–D). Compared to the hearts of control rats, periostin was expressed at higher levels in the fibrotic lesions of the hearts of test animals on D28PI (Fig. 4E and 4F). To assess the relationship between the levels of periostin and the representative fibrosis marker αSMA , we performed immunohistochemical staining of rat hearts. Although αSMA -positive cells were scarce in control hearts (Fig. 4G), the number of αSMA -positive fibroblasts in the hearts increased from D14PI to D28PI (Fig. 4H–K).

To gain further insight into the phenotype of cells infiltrating the hearts of EAM-induced rats, we conducted double immunofluorescence staining in the hearts taken at D14PI. Periostin-IB4 double-positive cells (arrowheads in Fig. 5A–C) were observed in inflammatory lesions, and ED1-positive macrophages were co-localized with periostin-positive cells (arrows in Fig. 5D–F). Furthermore, the periostin-expressing cells were co-localized with αSMA -positive fibroblasts (hollow arrows in Fig. 5G–I). These results suggest that fibroblasts and inflammatory cells are the main cell types expressing periostin in the fibrotic lesions of rats with EAM.

Although periostin has been implicated in various autoimmune diseases including peripheral polyneuropathy and myocardial infarction of mice [2, 6], this is the first study to show that periostin is upregulated in the hearts of EAM-induced rats, which model human myocarditis. Moreover, we found that periostin and αSMA , both of which are secreted by fibroblasts, were co-localized in the hearts of EAM-induced animals. These results suggest that upregulation of the extracellular matrix protein periostin is associated with early infiltration of inflammatory cells and subsequent fibrosis in autoimmune heart failure (Fig. 6).

We found that EAM-associated periostin upregulation was predominantly confined to inflammatory cells, consistent with our previous work showing that periostin levels significantly increased in spinal cord inflammatory cells and fibroblasts of mice with experimentally induced autoimmune encephalomyelitis [6]. EAM initiation is associated with heart infiltration of macrophages

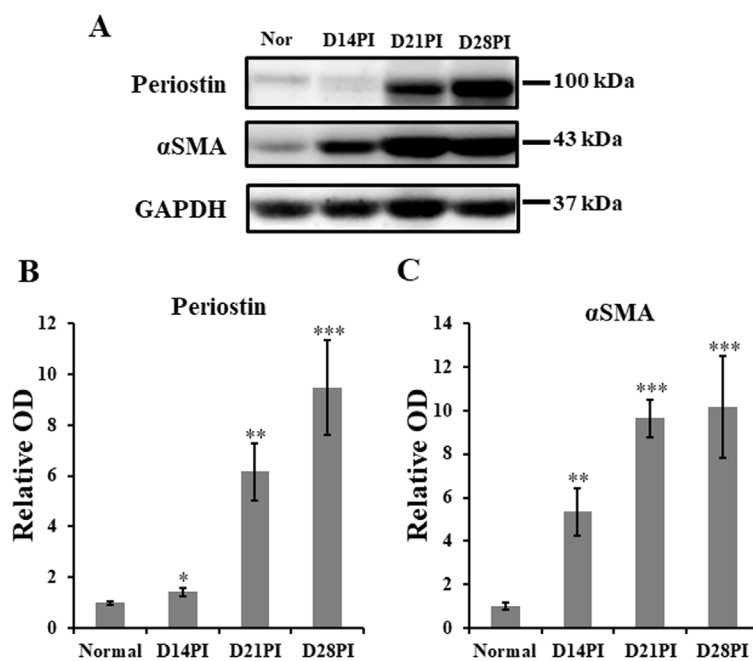


Fig. 3. Western blot analysis of periostin and alpha-smooth muscle actin (α SMA) protein levels in the hearts of control and experimental autoimmune myocarditis (EAM)-induced rats ($n=3$ per group). (A) Representative immunoblot showing periostin (~100 kDa), alpha smooth actin (α SMA; 43 kDa), and glyceraldehyde-3-phosphate dehydrogenase (GAPDH; 37 kDa) protein levels. Bar graphs show the quantification of periostin (B) and α SMA (C) protein levels normalized to GAPDH. Periostin and α SMA protein levels were significantly increased in the hearts of experimental autoimmune myocarditis (EAM)-induced rats. * $P<0.05$, ** $P<0.01$, *** $P<0.001$ vs. control.

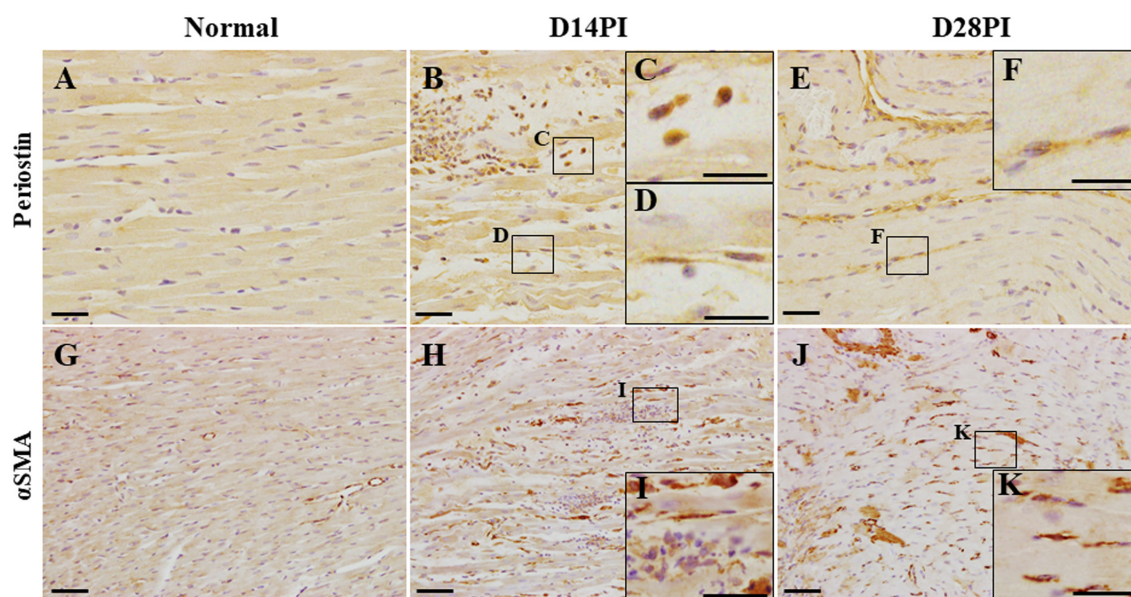


Fig. 4. Immunohistochemical staining of periostin and alpha-smooth muscle actin (α SMA) in the hearts of control and experimental autoimmune myocarditis (EAM)-induced rats. Periostin expression was detected in some inflammatory cells at day 14 post-immunization (C) and in fibroblasts (D and F) of EAM-affected hearts. However, only fibroblasts expressed alpha-smooth muscle actin (α SMA) in the hearts of EAM-affected rats (I and K). Tissues were counterstained with hematoxylin. (A, B, E, G, H, and J) Scale bars, 40 μ m. (C, D, F, I, and K) Scale bars, 20 μ m.

and autoreactive T cells [4]. After the acute inflammatory stage, excessive activation of cardiac fibroblasts triggers fibrosis and subsequent cardiac dysfunction [16]. Periostin neutralization or knockdown reduced glioma stem cell survival and suppressed cellular invasion and growth [18]. Thus, periostin upregulation in the heart may indicate inflammatory cell infiltration and increased risk for myocarditis. However, the precise mechanism underlying periostin-mediated fibrosis in the hearts of EAM-affected rats

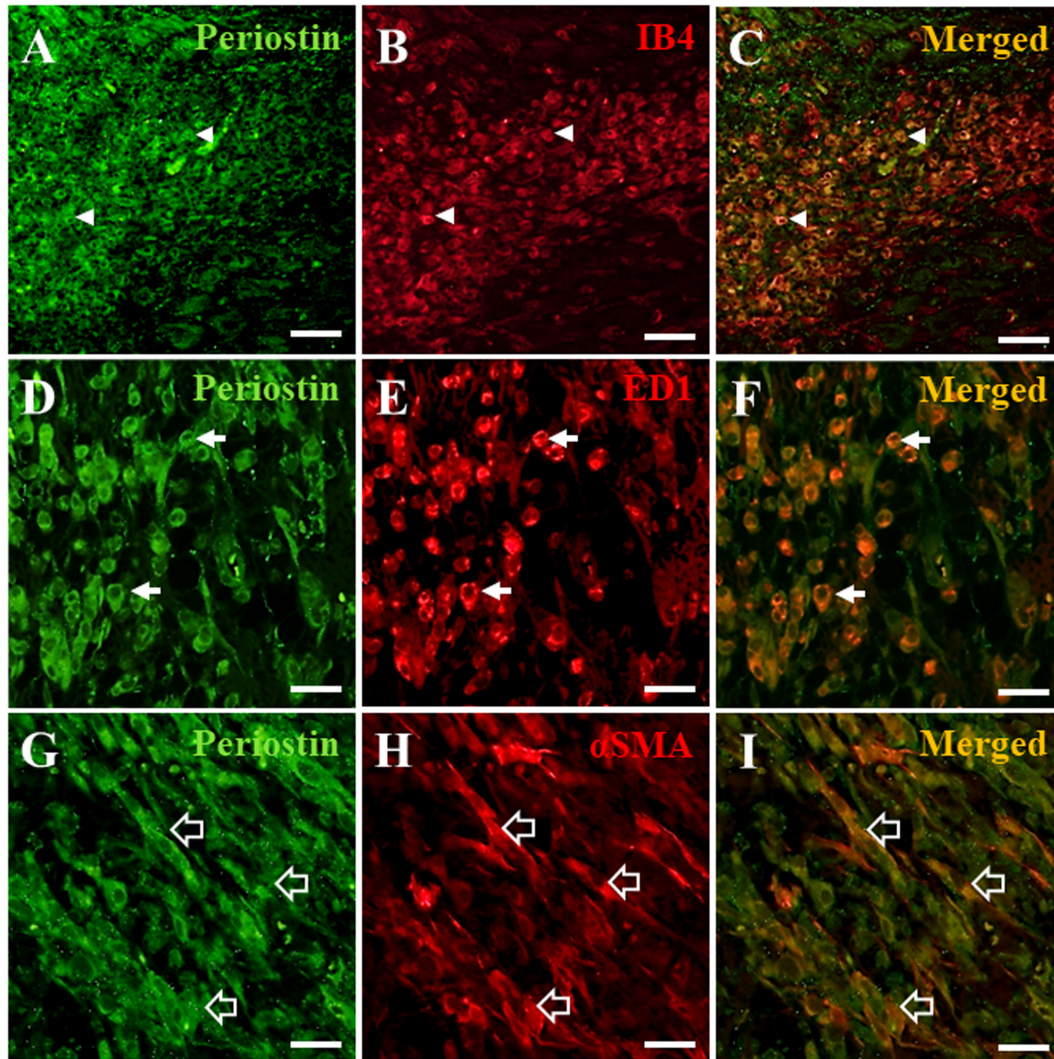


Fig. 5. Double immunofluorescence staining for periostin and either isolectin-B4 (IB4), ED1 or alpha-smooth muscle actin (α SMA) in experimental autoimmune myocarditis (EAM)-affected hearts (A–I). Periostin-positive inflammatory cells co-expressed isolectin-B4 (IB4) in EAM-affected hearts (arrowheads in A–C). Notably, macrophages doubly stained for periostin and ED1 (arrows in D–F). Some cardiac fibroblasts co-localized with α SMA and periostin (hollow arrows in G–I). (A–I) Scale bars, 20 μ m.

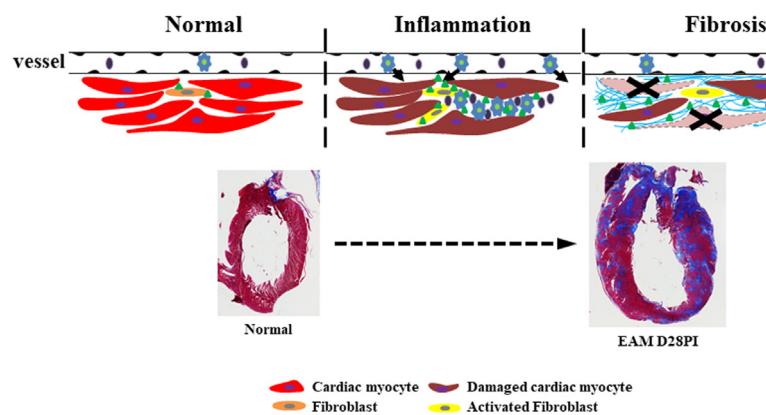


Fig. 6. Schematic illustration of periostin-mediated fibrosis in the hearts of experimental autoimmune myocarditis (EAM)-affected rats. When EAM is induced, macrophages infiltrate the heart. Infiltrated inflammatory cells secrete periostin, which activates cardiac fibroblasts and further promotes inflammatory cell infiltration. Activated fibroblasts express high levels of alpha-smooth muscle actin (α SMA) and periostin. Periostin accumulation results in the formation of fibrotic lesions in the heart, which could lead to heart failure.

requires further investigation.

In the present study, we found that α SMA levels were increased in EAM fibrotic lesions. α SMA is widely used as a marker for fibroblast activation, and its expression is induced in myocardial infarction by Prrx2-Wnt5a signaling and transforming growth factor (TGF)- β [3]. Furthermore, TGF- β and Smad signaling play important roles in fibrosis by regulating fibroblast activation and matrix deposition [17]. Notably, in an inflammatory dilated cardiomyopathy mouse model, TGF- β /Smad signaling induced myofibroblast development during heart tissue remodeling [5]. TGF- β has also been shown to promote periostin expression in primary osteoblasts [9]. Hence, we believe that α SMA upregulation in cardiac fibroblasts is essential for cardiac remodeling and fibrosis.

In conclusion, we demonstrated that periostin and α SMA are upregulated in the hearts of EAM-induced rats during disease initiation and progression. Our findings also suggest that periostin expression in infiltrating inflammatory cells and α SMA-positive fibroblasts plays an important role in cardiac fibrosis. Thus, periostin is a promising therapeutic target for myocarditis.

ACKNOWLEDGMENT. This work was supported by the 2020 education, research and student guidance grant funded by Jeju National University.

REFERENCES

1. Ahn, M., Lee, Y., Sim, K. B., Min, D. S., Matsumoto, Y., Wie, M. B., Shin, Y. G. and Shin, T. 2004. Increased expression of phospholipase D in the heart with experimental autoimmune myocarditis in Lewis rats. *Immunol. Invest.* **33**: 95–105. [Medline] [CrossRef]
2. Allard, D. E., Wang, Y., Li, J. J., Conley, B., Xu, E. W., Sailer, D., Kimpston, C., Notini, R., Smith, C. J., Koseoglu, E., Starmer, J., Zeng, X. L., Howard, J. F. Jr., Hoke, A., Scherer, S. S. and Su, M. A. 2018. Schwann cell-derived periostin promotes autoimmune peripheral polyneuropathy via macrophage recruitment. *J. Clin. Invest.* **128**: 4727–4741. [Medline] [CrossRef]
3. Bai, W. W., Tang, Z. Y., Shan, T. C., Jing, X. J., Li, P., Qin, W. D., Song, P., Wang, B., Xu, J., Liu, Z., Yu, H. Y., Ma, Z. M., Wang, S. X., Liu, C. and Guo, T. 2020. Up-regulation of paired-related homeobox 2 promotes cardiac fibrosis in mice following myocardial infarction by targeting of Wnt5a. *J. Cell. Mol. Med.* **24**: 2319–2329. [Medline] [CrossRef]
4. Barin, J. G., Rose, N. R. and Ciháková, D. 2012. Macrophage diversity in cardiac inflammation: a review. *Immunobiology* **217**: 468–475. [Medline] [CrossRef]
5. Blyszczuk, P., Müller-Edenborn, B., Valenta, T., Osto, E., Stellato, M., Behnke, S., Glatz, K., Basler, K., Lüscher, T. F., Distler, O., Eriksson, U. and Kania, G. 2017. Transforming growth factor- β -dependent Wnt secretion controls myofibroblast formation and myocardial fibrosis progression in experimental autoimmune myocarditis. *Eur. Heart J.* **38**: 1413–1425. [Medline]
6. Choi, Y., Kim, J., Ahn, M. and Shin, T. 2020. Upregulation of periostin in MOG-induced experimental autoimmune encephalomyelitis in mice. *Neurosci. Lett.* **715**: 134558. [Medline] [CrossRef]
7. Foot, N. C. 1933. The Masson Trichrome Staining Methods in Routine Laboratory Use. *Stain Technol.* **8**: 101–110. [CrossRef]
8. Frangiannidis, N. G. 2012. Matricellular proteins in cardiac adaptation and disease. *Physiol. Rev.* **92**: 635–688. [Medline] [CrossRef]
9. Horiuchi, K., Amizuka, N., Takeshita, S., Takamatsu, H., Katsura, M., Ozawa, H., Toyama, Y., Bonewald, L. F. and Kudo, A. 1999. Identification and characterization of a novel protein, periostin, with restricted expression to periosteum and periodontal ligament and increased expression by transforming growth factor beta. *J. Bone Miner. Res.* **14**: 1239–1249. [Medline] [CrossRef]
10. Huang, Y., Liu, W., Xiao, H., Maitikabili, A., Lin, Q., Wu, T., Huang, Z., Liu, F., Luo, Q. and Ouyang, G. 2015. Matricellular protein periostin contributes to hepatic inflammation and fibrosis. *Am. J. Pathol.* **185**: 786–797. [Medline] [CrossRef]
11. Izuhara, K., Nunomura, S., Nanri, Y., Ogawa, M., Ono, J., Mitamura, Y. and Yoshihara, T. 2017. Periostin in inflammation and allergy. *Cell. Mol. Life Sci.* **74**: 4293–4303. [Medline] [CrossRef]
12. Izumi, T., Takehana, H., Matsuda, C., Yokoyama, H., Kohno, K., Suzuki, K. and Inomata, T. 2000. Experimental autoimmune myocarditis and its pathomechanism. *Herz* **25**: 274–278. [Medline] [CrossRef]
13. Kim, J., Choi, Y., Ahn, M., Jung, K. and Shin, T. 2018. Olfactory dysfunction in autoimmune central nervous system neuroinflammation. *Mol. Neurobiol.* **55**: 8499–8508. [Medline] [CrossRef]
14. Kojima, T., Freitas, P. H., Ubaidus, S., Suzuki, A., Li, M., Yoshizawa, M., Oda, K., Maeda, T., Kudo, A., Saito, C. and Amizuka, N. 2007. Histochemical examinations on cortical bone regeneration induced by thermoplastic bioresorbable plates applied to bone defects of rat calvariae. *Biomed. Res.* **28**: 219–229. [Medline] [CrossRef]
15. Landry, N. M., Cohen, S. and Dixon, I. M. C. 2017. Periostin in cardiovascular disease and development: a tale of two distinct roles. *Basic Res. Cardiol.* **113**: 1. [Medline] [CrossRef]
16. Ma, Z. G., Yuan, Y. P., Wu, H. M., Zhang, X. and Tang, Q. Z. 2018. Cardiac fibrosis: new insights into the pathogenesis. *Int. J. Biol. Sci.* **14**: 1645–1657. [Medline] [CrossRef]
17. Meng, X. M., Nikolic-Paterson, D. J. and Lan, H. Y. 2016. TGF- β : the master regulator of fibrosis. *Nat. Rev. Nephrol.* **12**: 325–338. [Medline] [CrossRef]
18. Mikheev, A. M., Mikheeva, S. A., Trister, A. D., Tokita, M. J., Emerson, S. N., Parada, C. A., Born, D. E., Carnemolla, B., Frankel, S., Kim, D. H., Oxford, R. G., Kosai, Y., Tozer-Fink, K. R., Manning, T. C., Silber, J. R. and Rostomily, R. C. 2015. Periostin is a novel therapeutic target that predicts and regulates glioma malignancy. *Neuro-oncol.* **17**: 372–382. [Medline] [CrossRef]
19. Oh, H., Ahn, M., Matsumoto, Y. and Shin, T. 2013. Alternatively activated M2 macrophages increase in early stages of experimental autoimmune myocarditis in Lewis rats. *Korean J. Vet. Res.* **53**: 225–230. [CrossRef]
20. Shih, C. H., Lacagnina, M., Leuer-Bisciotti, K. and Pröschel, C. 2014. Astroglial-derived periostin promotes axonal regeneration after spinal cord injury. *J. Neurosci.* **34**: 2438–2443. [Medline] [CrossRef]
21. Zhou, W., Ke, S. Q., Huang, Z., Flavahan, W., Fang, X., Paul, J., Wu, L., Sloan, A. E., McLendon, R. E., Li, X., Rich, J. N. and Bao, S. 2015. Periostin secreted by glioblastoma stem cells recruits M2 tumour-associated macrophages and promotes malignant growth. *Nat. Cell Biol.* **17**: 170–182. [Medline] [CrossRef]